

# Improvement of electrical-resistivity model for polycrystalline films of metals with non-spherical Fermi surface: A case for Os films

S. L. Li,<sup>1</sup> Q. Y. Zhang,<sup>1,a)</sup> C. Y. Ma,<sup>1</sup> C. Zhang,<sup>2</sup> Z. Yi,<sup>2</sup> and L. J. Pan<sup>1</sup>

<sup>1</sup>Key Laboratory of Materials Modification by Laser, Ion and Electron Beams, and School of Physics and Opto-electronic Technology, Dalian University of Technology, Dalian 116024, China

<sup>2</sup>Science and Technology on Reliability and Environmental Engineering Laboratory, Beijing Institute of Spacecraft Environmental Engineering, Beijing 100094, China

(Received 7 February 2017; accepted 23 March 2017; published online 5 April 2017)

Osmium (Os) is a hexagonal-close-packed metal with a non-spherical Fermi surface that seriously deviates from the assumption in the Mayadas-Shatzkes electrical-resistivity model (MS model) for the size effects of polycrystalline films of metals due to electron scattering by grain boundaries. In this work, we studied the resistivity of the Os films with different thicknesses as a function of temperature in the range of 20 to 296 K. The electron scattering by the surface was found to be unimportant in the contributions to the size effects of resistivity of Os films with a sufficient thickness. Based on the first-principles calculations, an analytical equation was suggested for correction to the MS model and used for fitting the temperature-dependent resistivity of the Os films. The results show that correction to the MS model is necessary and the residual resistivity caused by the defects and impurities cannot be neglected. In addition, the inhomogeneity of resistivity in the direction perpendicular to the film surface was discussed under an assumption of parallel circuits. Published by AIP Publishing. [<http://dx.doi.org/10.1063/1.4979730>]

## I. INTRODUCTION

Osmium (Os), one of the noble metals, has particular properties useful for many applications, such as catalysis, fuel cells, electronics, and sensors.<sup>1,2</sup> Metallic Os is rather stable in air at room temperature. Due to the reaction of  $\text{Os} + 4\text{O} \rightarrow \text{OsO}_4$ , in which  $\text{OsO}_4$  is volatile, Os films are suggested to be useful for the fabrication of atomic oxygen (AO) sensors,<sup>3</sup> which are needed in investigations of a low-earth-orbit (LEO, 200–700 km) environment. Owing to its low efficiency of reaction with O atoms ( $\sim 3 \times 10^{-26}$  cm<sup>3</sup> per O atom),<sup>3</sup> Os is believed to be an ideal candidate because  $\mu\text{m}$ -thick Os films have been sufficient for the AO detection of the LEO environment for years, which is of significance for space science research. As a comparison, a  $\sim 20\text{-}\mu\text{m}$  Ag film just ensures the operation of the AO sensor for  $\sim 30$  days.<sup>4</sup> In the AO detection of the LEO environment, the electrical resistance of sensors with a patterned circuit is usually used for the estimation of the AO density in the atmosphere because its value varies with the loss of Os films.<sup>3</sup> Therefore, the electrical resistivity, which is a function of the film thickness and temperature, is a parameter crucial for the determination of AO doses reacting with the Os films.

Electrical resistance originates from the electron momentum loss along the direction of current flow. Matthiessen's rule showed that the electrical resistivity of a metal is a function of temperature and densities of defects and impurities in the metal. The temperature-dependent resistivity is due to electron scattering by lattice vibration (phonons). For a polycrystalline film, the temperature-dependent resistivity usually depends on the film thickness because electrons could be

scattered by the surface (interface) and the grain boundaries.<sup>5</sup> Therefore, the values of resistivity for polycrystalline films at a given temperature are thickness-dependent. These phenomena are referred to as size effects of film resistivity.<sup>5</sup> Fuchs<sup>6</sup> and Sondheimer<sup>7</sup> (FS) used a specularly scattered parameter,  $p$ , to denote the fraction of electrons that are specularly scattered from the surfaces, with  $(1-p)$  denoting the fraction scattered diffusely; thus, the dependence of resistivity on the film thickness ( $h$ ) was written as  $\rho_{\text{FS}} = \rho_{\text{B}}/f_{\text{FS}}(h)$ , in which  $\rho_{\text{B}}$  is the resistivity of the bulk material and  $f_{\text{FS}}(h)$  is given by

$$f_{\text{FS}}(h) = 1 - \frac{3}{2k}(1-p) \int_1^\infty \left( \frac{1}{t^3} - \frac{1}{t^5} \right) \frac{1 - \exp(-kt)}{1 - p \exp(-kt)} dt, \quad (1)$$

where  $k = h/\lambda$  is a reduction thickness by the mean free path (MFP) of electrons ( $\lambda$ ). This equation is usually referred to as the FS model. Mayadas and Shatzkes<sup>8</sup> (MS) introduced a reflection coefficient,  $r$ , for the discussion of electron scattering by grain boundaries.  $r$  represents the fraction of electrons that are reflected at grain boundaries perpendicular to the direction of current flow, and then  $(1-r)$  corresponds to the electrons transmitted. Then, the resistivity of polycrystalline films is written as a function of the in-plane (lateral) grain size  $D$  by  $\rho_{\text{MS}} = \rho_{\text{B}}/f_{\text{MS}}(D)$ , in which  $f_{\text{MS}}(D)$  is

$$f_{\text{MS}}(D) = 1 - \frac{3}{2}\alpha + 3\alpha^2 - 3\alpha^3 \ln \left( 1 + \frac{1}{\alpha} \right), \quad (2)$$

where  $\alpha = \frac{\lambda}{D} \frac{r}{1-r}$ . This model is usually referred to as the MS model. Taking into account the MS and FS models without the consideration of their interaction (FS + MS model),<sup>9</sup> the total resistivity of a metallic film is

<sup>a)</sup>Author to whom correspondence should be addressed. Electronic mail: qyzhang@dlut.edu.cn

$$\rho = \rho_B + \Delta\rho_{FS} + \Delta\rho_{MS}, \quad (3)$$

where  $\Delta\rho_{FS} = \rho_{FS} - \rho_B$  and  $\Delta\rho_{MS} = \rho_{MS} - \rho_B$ . Another model allowing interaction between the two scattering mechanisms was also suggested by Mayadas and Shatzkes<sup>8</sup> and referred to as the Mayadas-Shatzkes surface (MSS) model in the literature.<sup>9</sup> The FS model was found to play an important role in contributions to the size effect of resistivity only when the thickness of film is sufficient thin.<sup>9</sup> As for the MS model, the analytical equation (2) was given by assuming a spherical Fermi surface<sup>8</sup> and thus would be failed in some metals when the Fermi surface is far from the assumption. For example, tungsten (W) is a body-center-cubic (bcc) metal, with a Fermi surface similar to that of Mo.<sup>10</sup> The first-principles calculations showed that the Fermi surface for some bcc metals, such Mo and W, is rather complex and far from the assumption of the spherical Fermi surface.<sup>10,11</sup> Therefore, improvement for these metals is needed if the MS model is used for the study of the resistivity size effects. In fact, a systematic deviation from the theoretical results has been observed in the study by Choi *et al.*<sup>12</sup> on polycrystalline W films. However, an analytical equation for the improvement of the MS electrical-resistivity model is still unavailable in the literature.

In this work, polycrystalline Os films with different thicknesses were prepared for the study of the size effect of resistivity. The electron scattering by the surface was discussed using the FS model and found to be unimportant for the size effect of resistivity, and the temperature-dependent resistivity was found to deviate from the results predicted by the MS model. Based on the analysis of the Fermi surface that was calculated using the CASTEP code, an analytical equation was suggested to correct the MS model for fitting the experimental data of the Os films. In addition, the inhomogeneity of resistivity in the direction perpendicular to the film surface was discussed under an assumption of parallel circuits.

## II. EXPERIMENTAL METHODS

The polycrystalline Os films with different thicknesses were prepared by a magnetron sputtering method using substrates of 1.5-mm thick fused quartz with a size of  $30 \times 20$  mm.<sup>13</sup> The film thickness was determined by checking the change in the mass of the sample before and after the deposition of Os films using a balance with a sensitivity of 0.1 mg, which leads to an uncertainty of  $\sim 5$  nm for Os films. For the Os films deposited for specific lengths of time, the film thicknesses were determined to be 285, 551, 876, 1259, and 1535 nm in good agreement with the results of cross-sectional samples determined by scanning electron microscopy (SEM, Hitachi S-4800). The inhomogeneity in the film thickness was evaluated by a standard four-probe method *via* the measurement of sheet resistance at 12 positions over the film surface, showing that the average errors are less than 5.5%. X-ray diffraction (XRD, Bruker D8 DISCOVER) analysis revealed that the Os films have a hexagonal-close-packed (hcp) structure with a preferred orientation of (001).<sup>12</sup> The measurement by atomic force microscopy (AFM, Benyuan

CSPM5000) showed that the root-mean-square (rms) roughness is smaller than 1.5 nm. No impurity was observed in the examination by x-ray energy dispersive (EDX) spectroscopy, indicating that the purity of Os films is rather high. More details for the preparation and characterization of the Os films can be found in our previous article.<sup>13</sup>

The room-temperature resistivity ( $\rho_F$ ) of the Os films was found to be thickness-dependent and could be fitted by  $\rho_F = 13.0 + 1.74/h$  ( $\mu\Omega\text{cm}$ ),<sup>13</sup> in which  $h$  is in  $\mu\text{m}$ . Therefore, the size effects of resistivity were further studied in this work by measuring the resistivity values of the Os films as a function of temperature. To measure the sheet resistance of the Os films, four electrodes of copper were connected to the surface of each sample using a kind of conducting glue containing Ag particles. The measurement was conducted using a four-probe testing system (Agilent B2900A) at temperatures ranging from 296 down to 20 K. The sheet resistance was determined by linearly fitting the current-voltage ( $I$ - $V$ ) curves, producing relative errors within  $1.0 \times 10^{-4}$ . The grain sizes in the Os films were estimated by the Scherrer method using the full width at half maximum (FWHM) of the diffraction peaks.

To study the electronic structure and the Fermi surface, the first-principles calculations were carried out using the code CASTEP<sup>14</sup> based on density functional theory (DFT). Norm-conserving pseudo-potential,<sup>15</sup> with the electronic configuration of  $4f^{14}5d^66s^2$ , and plane-wave expansion of wave functions were used for the calculations. The generalized gradient approximation (GGA) in the Perdew–Burke–Erzerhof scheme<sup>16</sup> was used for the description of the exchange and correlation potential. The interaction between ions and valence electrons was described by the projector-augmented wave (PAW) potential method. The optimization of lattice parameters was conducted using  $a = 2.744 \text{ \AA}$  and  $c = 4.329 \text{ \AA}$ , which were optimized by Xu and Verstraete<sup>17</sup> and were in good agreement with the data that are determined in experiments. The optimized parameters were  $a = 2.84 \text{ \AA}$  and  $c = 4.43 \text{ \AA}$ , which are  $\sim 3\%$  higher than those obtained by Xu and Verstraete and thus cannot have a serious impact on the electronic structure and the shapes of the Fermi surface. The  $k$ -point set mesh was chosen to be  $50 \times 50 \times 30$ . After careful testing, the cutoff energy was set to 1000 eV. The calculation was stopped at a force smaller than 0.01 eV per atom.

## III. RESULTS AND DISCUSSION

The MFP of electrons is a crucial factor for the study of resistivity size-effects of polycrystalline films. In this work, the MFP function ( $\lambda$ ) of electrons was calculated using bulk resistivity ( $\rho_B$ ) and a constant  $\lambda_{RT} \times \rho_{RT}$ , in which  $\lambda_{RT}$  and  $\rho_{RT}$  are the values at room temperature. The bulk resistivity of Os had been well studied as a function of temperature in experiment<sup>18–20</sup> and in theory.<sup>17</sup> Similar to other normal metals, Os has the bulk resistivity very close to a linear function at temperatures ( $T$ ) above 50 K, as shown in Fig. 1. Below 15 K, the temperature dependence could be fitted by  $\rho = \rho_0 + AT^2 + BT^5$ ,<sup>17</sup> where the three terms are due to electron scattering by impurities, other electrons, and photons. Gall's<sup>10</sup> first-principles calculations showed that the value of  $\lambda_{RT} \times \rho_{RT}$  is  $6.41 \times 10^{-6} \mu\Omega\text{cm}^2$  for the current flow in the

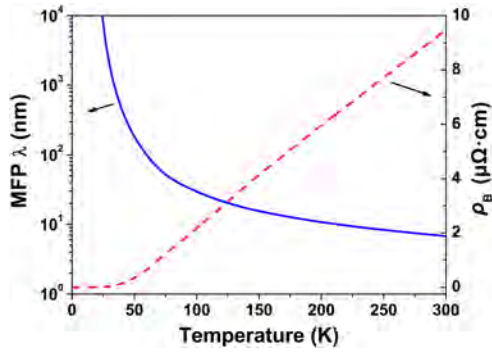


FIG. 1. MFP function of electrons (solid line) and bulk resistivity (dashed line) for the Os with a hcp structure. The bulk resistivity was calculated by interpolating the data taken from the plot in the study by Xu and Verstraete.<sup>17</sup>

plane perpendicular to the [001] direction of the hcp structure. By B-spline interpolating the data taken from the plot in the study by Xu and Verstraete,<sup>17</sup> we determined the MFP function of electrons below 300 K, as shown in Fig. 1.

Using the MFP function, we calculated the surface-scattering contributions to the resistivity of Os films using the FS model with  $p=0.2$ , as shown in Fig. 2. For the Os films with the specific thicknesses, surface-scattering leads to an increase in the resistivity ( $\Delta\rho_{FS}$ ), which strongly depends on the film thickness and slowly varies at the temperatures ranging from 20 to 300 K. With the increase in the film thickness, the values of  $\Delta\rho_{FS}$  sharply decrease. For the films with thicknesses larger than 200 nm,  $\Delta\rho_{FS}$  is decreased to the values generally below  $0.1 \mu\Omega \text{ cm}$ , which is much smaller than that of the resistivity observed in experiment. Therefore, we are convinced that electron scattering by the surface is unimportant in the contributions to the resistivity in this work because the Os films are sufficiently thick.

In the MS model, the grain size is used as a parameter to calculate the film resistivity due to the electron scattering by grain boundaries. However, this parameter is not independent in the MS model because it acts with the reflection coefficient,  $r$ , which is unknown and is usually determined by fitting experimental data. Therefore, it is much more important to know the dependence of the grain size on the film thickness than to accurately measure the actual sizes of grains in films. As a matter of fact, it is impossible to accurately determine the actual sizes of grains in polycrystalline

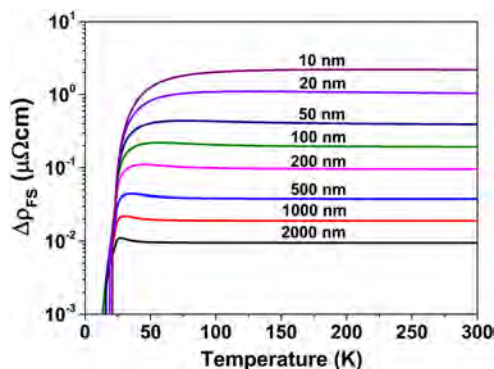


FIG. 2.  $\Delta\rho_{FS}$  values calculated using the FS model with  $p=0.2$  for Os films with the specific thicknesses.

films because the grain size is not a constant and varies layer by layer from the bottom to the top. As such, transmission electron microscopy (TEM) is not a right measure to determine the average sizes of grains in  $\mu\text{m}$ -thick films because the values of grain sizes strongly depend on TEM sample preparation. In this work, therefore, the average sizes of grains in the Os films were estimated by the Scherrer method using the FWHM values of the XRD peaks.<sup>13</sup> The grain sizes were found to be increasing with the increase in the film thickness, as shown in Fig. 3, and could be fitted by

$$D = D_0 + \Delta D(1 - e^{-h/h_0}), \quad (4)$$

in which  $D_0=27.0 \text{ nm}$ ,  $\Delta D=17.5 \text{ nm}$ , and  $h_0=668 \text{ nm}$  were determined in this work. This equation enabled the grain sizes to increase with the increase in the film thickness. In the study by Choi *et al.*<sup>12</sup> on polycrystalline W films, a quadratic function was used for fitting the dependence of the grain size on the film thickness. This quadratic polynomial is valid for the film thickness changing in a relatively small range<sup>12</sup> but will lead to the decrease in the grain size of the films with a sufficient thickness.

Using the MFP function and the grain sizes, the experimental data of resistivity for the Os films were fitted as a function of temperature using the FS + MS model by calculating the minimum of the sum of squared errors (SSEs), which is a standard method widely used in the study of size effects of film resistivity.<sup>9,12</sup> As surface-scattering is not important,  $p=0.2$  was used for calculating the contributions of the FS model. For the best fits, the calculation results were found to deviate from the experimental data for all the films, as shown in Fig. 4, in which the dashed lines are the best fits using the FS + MS model. Furthermore, using other  $p$  values or using the MSS model cannot lead to an obvious improvement in the deviation. A similar deviation was also observed in the study by Choi *et al.*<sup>12</sup> on polycrystalline W films. Therefore, we are convinced that this deviation is probably due to the problems in the MS model because the hcp Os has a complex Fermi surface<sup>17,21</sup> much different from Mayadas-Shatzkes's assumption. For this propose, the code CASTEP was used to investigate the electronic structure and the Fermi surface of Os.

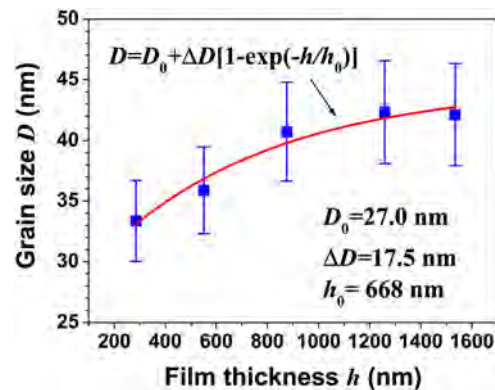


FIG. 3. Grain sizes plotted as a function of the film thickness for the Os films. The error bars indicate the uncertainty of calculations due to the XRD data.

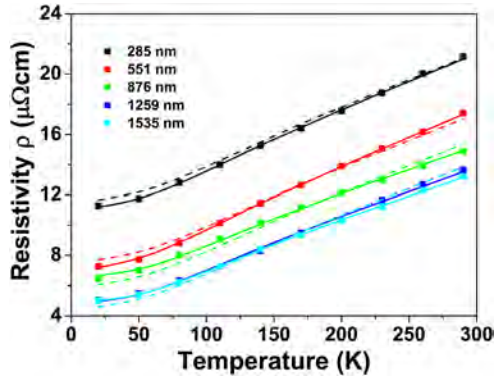


FIG. 4. Best fits to the experimental data (solid dots) of resistivity for the Os films with the given thicknesses using the FS + MS model (dashed line) and the improved MS model (solid line).

Fig. 5(a) shows the electronic structure and density of state (DOS) of Os with a hcp structure. Though its electronic structure is similar to that of other metals, the value of the DOS at the level of Fermi energy ( $E_F$ ) is relatively low. On the other hand, there are many bands crossing the Fermi level, which is an indication that the Fermi surface consists of the electrons from multiple bands, such as the  $6s$  and  $5d$  bands. Fig. 5(b) shows the views of the Fermi surface projected from  $[100]$ ,  $[001]$ , and the incline directions. Much differing from alkali metals and the metals such as Cu, Ag, and Au, in which the Fermi surface is generally sphere-like, the Fermi surface for Os has three individual bands, which were evidenced by the calculations in the study by Xu and

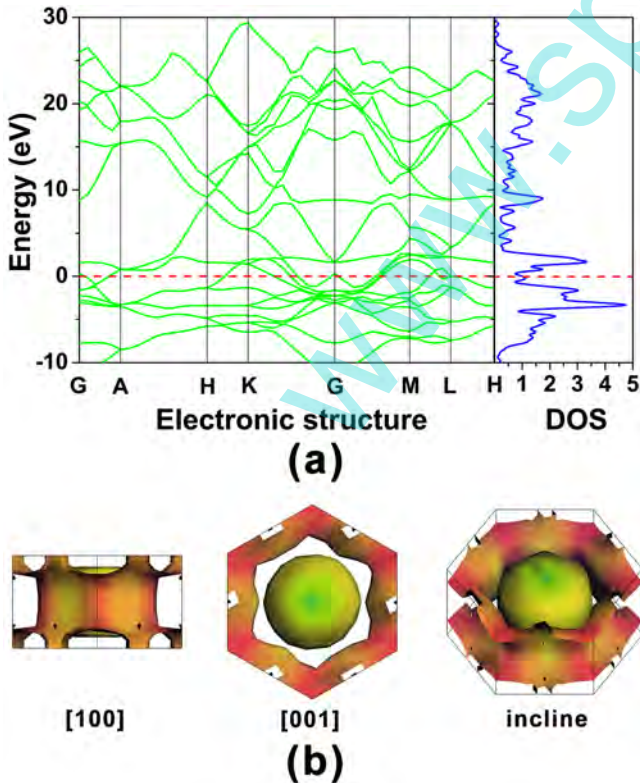


FIG. 5. (a) Electronic structure and density of state (DOS) and (b) Fermi surface for the Os metal with a hcp structure. The dashed line in the figures indicates the Fermi level.

Verstraete<sup>17</sup> on the inclusion of the spin-orbit coupling and by Koudela *et al.*<sup>21</sup> using the precise density functional calculations. The first and the second bands are complex polyhedrons with six-fold symmetry, differing from the inner “electron star” for Ru.<sup>10</sup> The first band is small and is enclosed by the second band. Similar to the “hole ring” for Ru,<sup>10</sup> the outer part is much complex and can be roughly regarded as a “hexagonal ring” with the ledges extending towards the outside until the boundary of the Brillouin zone. Due to the complexity of the Fermi surface, the Fermi velocity ( $v_F$ ) varies in one order of magnitude and strongly depends on the position over the surface. As a comparison, the Fermi velocity for Cu is relatively constant over most of the surface.<sup>10</sup>

Based on the above results of the first-principles calculations, we have a simple discussion on the MS model below. According to the solid state theory,<sup>8,22</sup> the electrical conductivity of metals is written as

$$\sigma = \frac{e^2}{4\pi^3} \int \frac{\tau v_x^2}{|\nabla_{\mathbf{k}} E|} dS_F, \quad (5)$$

where  $e$  is the charge of electrons,  $\tau$  is the relaxation time of electrons in a perfect metal, and  $v_x$  is the velocity along the direction of current flow. The integration is over the total area of the Fermi surface ( $S_F$ ). The grain-boundary scattering was taken into account by Mayadas and Shatzkes<sup>8</sup> using an effective relaxation time ( $\tau^*$ ), which could be calculated by

$$\frac{1}{\tau^*} = \frac{1}{\tau} + 2F(|k_x|), \quad (6)$$

with

$$F(|k_x|) = \frac{\alpha k_F}{2\tau |k_x|}. \quad (7)$$

Under the assumption of a spherical Fermi surface, the constant  $v_F$  produces an analytical form similar to Eq. (2).<sup>8</sup> Under the first approximation, the inner “electron polyhedrons” for Os could be regarded as a sphere-like Fermi surface. Therefore, the MS model is an acceptable approximation for the inner contributions to the resistivity. However, the outer “hexagonal ring” cannot be approximated by the MS model anymore. In fact, it is rather difficult to give an analytical form for the outer contributions to the resistivity, even if the shape is largely simplified. By exploration of the integration and the experimental data, the values of resistivity for the Os films were found to be well fitted using a correction to the MS model below

$$\Delta\rho_{ZL} = \rho_R + \frac{\beta}{\lambda}, \quad (8)$$

in which  $\rho_R$  and  $\beta$  are the fitting parameters. Then, the resistivity of Os films is written as

$$\rho_{MS+ZL} = \rho_{MS} + \Delta\rho_{ZL}. \quad (9)$$

Using the improved MS model and the FS model with  $\rho = 0.2$ , we fitted the experimental data by the SSE method.

The best fits were found much better than that obtained using the MS + FS model, as the solid lines shown in Fig. 4, and the parameters for the best fits are listed in Table I. The  $\rho_R$  values were observed to be close to each other for most of the Os films. Following Matthiessen's rule, this parameter is probably in association with the residual resistivity, which is related to the densities of defects and impurities in the films, and thus being different from sample to sample. In comparison with the materials fabricated using the metallurgy method, quite a large amount of defects would be created during film growth, including vacancies, interstitials, and dislocations. These defects are not easy to be removed due to the existence of film stresses and the relatively low temperature for film growth and post-annealing; thus, their effects are detectable in the measurement of film resistivity. However, this residual resistivity had never been taken into account in the previous studies related to the size effects of film resistivity. For example, the systematical deviation in the study by Choi *et al.*<sup>12</sup> on nanometric-polycrystalline W films was attributed to the reasons like multiple relevant length scales for bulk resistivity and quantum size effects for electrons, without the consideration of the residual resistivity as well as the influence of the non-spherical Fermi surface on the MS model, which is taken into account in this work using the other parameter,  $\beta$ . The good agreement between the fitting curves and the experimental data suggests that the improved MS model is successful for the resistivity size-effects of the Os films and is probably useful for studying the resistivity size effects of polycrystalline films of other metals.

As mentioned above, the lateral sizes of grains in a polycrystalline film are varying layer by layer with the decrease in the film depth from the bottom to the top. In other words, the depth profile of grain sizes is inhomogeneous. This inhomogeneity in grain sizes was further demonstrated by our SEM observation of the cross-sectional samples, as shown in Fig. 6(a). Similar to most of the polycrystalline films, these Os films consisted of columnar grains with the sizes increasing from the bottom to the top. As such, according to the MS model, the resistivity values for the Os film with a specific thickness should be decreasing layer by layer with the decrease in the depth from the bottom to the top. In this work, the Os films with different thicknesses were observed to have a similar morphology with grain sizes close to each other at the same distance to the substrates. Therefore, we are able to study the depth profile of the resistivity using a group of Os films because surface-scattering is unimportant in these Os films. Three samples of Os films with thicknesses of 285, 551, and 1259 nm were selected for this purpose and

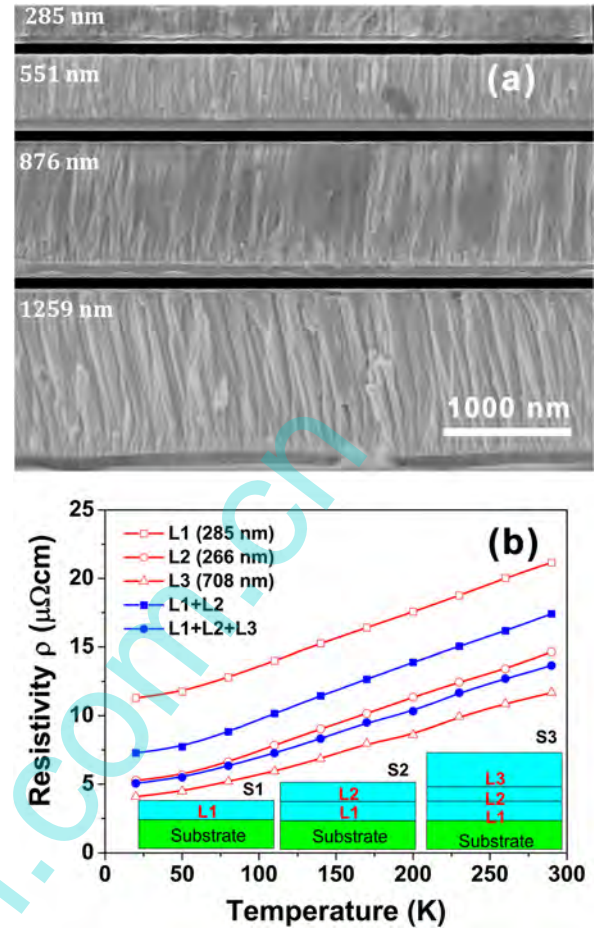


FIG. 6. (a) SEM images of Os-film cross-sectional samples with the given thicknesses. (b) Layered values of resistivity in the Os films calculated under an assumption of parallel circuits. The layered structures are shown in the insets in (b).

were labeled as S1, S2, and S3, respectively. We regarded these samples as the layered samples, as shown in the inset in Fig. 6(b), and supposed that L1, L1 + L2, and L1 + L2 + L3 have the same thickness and resistivity as S1, S2, and S3, respectively. As such, it is not difficult to calculate the resistivity value of each layer based on parallel circuits. As shown in Fig. 5(b), the calculation results clearly show that the resistivity value in each layer decreases from L1 to L3, thus demonstrating the inhomogeneity of resistivity in the direction perpendicular to the film surface.

#### IV. CONCLUSIONS

In conclusion, the resistivity of Os films was studied as a function of temperature ranging from 20 to 296 K. For the Os films with thicknesses of 285 to 1535 nm, the increase in resistivity due to electron scattering by the surface is smaller than  $0.1 \mu\Omega \text{ cm}$  and the values sharply decrease with the increase in the film thickness, thus is unimportant for the size effects of resistivity. The first-principles calculations showed that the Fermi surface for Os consists of two inner "electron polyhedrons" and one outer "hexagonal ring," thus seriously deviating from the assumption of the spherical Fermi surface in the MS model. An analytical equation was suggested for correction to the MS model, and then the

TABLE I. Parameters for the best fits using the improved MS model.

$h$ (nm)	$D$ (nm)	$p$	$r$	$\rho_R$ ( $\mu\Omega \text{ cm}$ )	$\beta$ ( $\times 10^{-7} \mu\Omega \text{ cm}^2$ )
285	33.4	0.2	0.80	0.96	2.1
551	35.9	0.2	0.73	0.78	4.8
876	40.7	0.2	0.73	0.94	-7.9
1259	42.2	0.2	0.66	0.98	-5.4
1535	42.2	0.2	0.69	0.44	-8.3

experimental data of resistivity for the Os films were well fitted. The results showed that the residual resistivity cannot be neglected because a large amount of defects and impurities would be created during film growth. Under an assumption of parallel circuits, the inhomogeneity of resistivity in the direction perpendicular to the film surface was demonstrated using a group of Os films, indicating that the values of resistivity decrease in the layers from the bottom to the top. This study may help in the study of the resistivity size-effects of polycrystalline films of other metals with non-spherical Fermi surfaces.

## ACKNOWLEDGMENTS

This research was supported by the Basic Research Project for the Key Laboratory of Liaoning Province of China (Grant No. LZ2014006) and the Fundamental Research Funds for the Central Universities of China (Grant Nos. DUT16ZD207 and DUT16-LAB01). One of the authors, Professor L. J. Pan, is thankful for financial support from the National Natural Science Foundation of China under Grant No. 11274055.

<sup>1</sup>J. Hämäläinen, T. Sajavaara, E. Puukilainen, M. Ritala, and M. Leskelä, *Chem. Mater.* **24**, 55 (2012).

<sup>2</sup>W. M. Haynes, *CRC Handbook of Chemistry and Physics*, 91st ed. (Internet Version 2011 and CRC Press/Taylor and Francis, Boca Raton, 2011).

<sup>3</sup>X. P. Liu, J. Y. Tong, S. H. Xiang, and Z. Jia, *Spacecr. Environ. Eng.* **27**, 300 (2010).

<sup>4</sup>Y. Cheng, X. Chen, and T. Sheng, *Adv. Space Res.* **57**, 281 (2016).

<sup>5</sup>D. Josell, S. H. Brongersma, and Z. Tókei, *Annu. Rev. Mater. Res.* **39**, 231 (2009).

<sup>6</sup>K. Fuchs, *Proc. Cambridge Philos. Soc.* **34**, 100 (1938).

<sup>7</sup>E. H. Sondheimer, *Adv. Phys.* **1**, 1 (1952).

<sup>8</sup>A. F. Mayadas and M. Shatzkes, *Phys. Rev. B* **1**, 1382 (1970).

<sup>9</sup>T. Sun, B. Yao, A. P. Warren, K. Barmak, M. F. Toney, R. E. Peale, and K. R. Coffey, *Phys. Rev. B* **81**, 155454 (2010).

<sup>10</sup>D. Gall, *J. Appl. Phys.* **119**, 085101 (2016).

<sup>11</sup>D. Choi, C. S. Kim, D. Naveh, S. Chung, A. P. Warren, N. T. Nuhfer, M. F. Toney, K. R. Coffey, and K. Barmak, *Phys. Rev. B* **86**, 045432 (2012).

<sup>12</sup>D. Choi, X. Liu, P. K. Schelling, K. R. Coffey, and K. Barmak, *J. Appl. Phys.* **115**, 104308 (2014).

<sup>13</sup>S. L. Li, C. Y. Ma, Q. Y. Zhang, X. P. Liu, C. Zhang, and Z. Yi, *Surf. Coat. Technol.* **282**, 1 (2015).

<sup>14</sup>M. Segall, P. Lindan, M. Probert, C. Pickard, P. Hasnip, S. Clark, and M. Payne, *J. Phys.: Condens. Matter* **14**, 2717 (2002).

<sup>15</sup>D. R. Hamann, M. Schlüter, and C. Chiang, *Phys. Rev. Lett.* **43**, 1494 (1979).

<sup>16</sup>J. P. Perdew, K. Burke, and M. Ernzerhof, *Phys. Rev. Lett.* **77**, 3865 (1996).

<sup>17</sup>B. Xu and M. J. Verstraete, *Phys. Rev. B* **87**, 134302 (2013).

<sup>18</sup>R. W. Powell, R. P. Tye, and M. J. Woodman, *Platinum Met. Rev.* **6**, 138 (1962).

<sup>19</sup>J. T. Schriempf, *Solid State Commun.* **6**, 873 (1968).

<sup>20</sup>E. M. Savitskii, V. P. Polyakova, N. B. Gorina, and N. R. Roshan, *Physical Metallurgy of Platinum Metals* (Mir, Moscow and New York, 1978).

<sup>21</sup>D. Koudela, M. Richter, A. Möbius, K. Koepf, and H. Eschrig, *Phys. Rev. B* **74**, 214103 (2006).

<sup>22</sup>J. Callaway, *Quantum Theory of the Solid State* (Academic Press, New York, San Francisco, and London, 1976).